C. R. Physique 3 (2002) 493–500

Solides, fluides : propriétés électroniques et optiques/*Solids, fluids: electronic and optical properties*
(Surfaces, interfaces, films/*Surfaces, interfaces, films*)

DOSSIER

PHOTONIQUE MOLECULAIRE : MATÉRIAUX, PHYSIQUE ET COMPOSANTS

MOLECULAR PHOTONICS: MATERIALS, PHYSICS AND DEVICES

Luminescence induced by a scanning-tunneling microscope as a nanophotonic probe

Fabien Silly [1], Fabrice Charra *

CEA-Saclay, Service de physique et chimie des surfaces et interfaces, DSM-DRECAM, 91191 Gif-sur-Yvette cedex, France

Accepted 1 March 2002

Note presented by Guy Laval.

Abstract The luminescence of nanostructured systems can be excited highly locally by the tip of a Scanning Tunneling Microscope (STM). We first present briefly the principles of this STM-induced luminescence. Then we present a review of selected results in STM-induced luminescence from the point of view of nano-scale photonics. We illustrate various contrast mechanisms with different examples of nanostructured systems. ***To cite this article: F. Silly, F. Charra, C. R. Physique 3 (2002) 493–500.*** © 2002 Académie des sciences/Éditions scientifiques et médicales Elsevier SAS

scanning tunneling microscopy / scanning tunneling luminescence / nanophotonics / plasmons

Luminescence induite par un microscope à effet tunnel comme sonde nanophotonique

Résumé La luminescence de systèmes nanostructurés peut être induite de manière très localisée par la pointe d'un microscope à effet tunnel (STM). Après avoir résumé les principes d'une telle luminescence induite par STM, nous passons en revue des résultats expérimentaux récents dans ce domaine, du point de vue de la photonique à l'échelle nanoscopique. Nous illustrons différents mécanismes de contraste sur plusieurs examples de systèmes nanostructurés. ***Pour citer cet article : F. Silly, F. Charra, C. R. Physique 3 (2002) 493–500.*** © 2002 Académie des sciences/Éditions scientifiques et médicales Elsevier SAS

microscopie à effet tunnel / luminescence à effet tunnel / nanophotonique / plasmons

1. Introduction

Optical spectroscopy techniques are essential tools for probing the electronic and photophysical properties of condensed matter. A wide range of spectroscopic methods is available, including absorption-,

* Correspondence and reprints.
E-mail address: fabrice.charra@cea.fr (F. Charra).

S1631-0705(02)01328-2/FLA

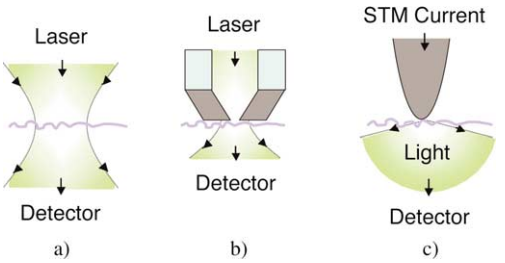

Figure 1. Schematic representations of (a) far-field optical microscopy (e.g. confocal microscopy), (b) scanning near-field optical microsopy (SNOM) based on metal-coated fiber-tip probes, and (c) STM-induced luminescence.

emission-, excitation-, polarization- and ultrafast time-resolved-spectroscopy. However, the wavelength-limited spatial resolution in far-field optical techniques prevents local nanometer-scale photophysical studies (see Fig. 1(a)). This is a severe limitation considering the new trends for nanoscale-structured functional opto-electronic materials such as advanced molecular materials. Several approaches have been adopted to circumvent this problem in order to excite locally nanostructured objects. A first *all-optical* approach takes advantage of near-field optical scanning probe techniques originally developed for high-resolution optical microscopy. Typically, the light scattered through a sub-wavelength sized aperture at the free end of an optic fiber is used as a secondary light source, scanned close to the studied surface (see Fig. 1(b)). The resolution is then limited by the optical skin depth of the aperture material, typically several tens of nanometers. This paper deals with an alternative approach which combines an optical detection system and a Scanning Tunneling Microscope (STM, see Fig. 1(c)). It consists in taking advantage of the extreme localization of the tunnel current for exciting locally nano-structured objects with energies in the optical range. The locally-excited luminescence can then be analyzed in the far-field. In fact, when the STM junction is biased with a voltage V_{T} between 1 and a few volts, the current at the tunnel junction behaves as a highly localized electro-magnetic source at frequency $\omega \leqslant eV_{\mathrm{T}}/\hbar$ in the optical range [1,2]. The resulting luminescence can provide photophysical information with an unparalleled spatial resolution, below 1 nm. However, the analysis is complicated since contrast, i.e. spatial variation of luminescence characteristics, not only occurs through local variations of optical parameters but also from electronic structure which may influence the spectral properties of the exciting source, or the mechanisms and efficiency of electron–photon conversion. Interpretations of photon maps must thus include a careful analysis of contrast origins.

In this review we present selected results of STM-induced luminescence from the point of view of nano-scale photophysics. We first present briefly the principles of STM-induced luminescence. Then we illustrate various contrast mechanisms with different examples of nanostructured systems.

2. STM techniques

Light emission from a tunnel junction was first observed in metal-oxide–metal systems [2]. Following the advances in scanning probe microscopy, photon emission was observed in a STM with relatively high quantum efficiencies [3] and with molecular-scale imaging resolution [4]. The possibility of achieving a chemical contrast through this technique has been demonstrated for carbon clusters on silicon [5] and tip-induced surface chemical modifications [6]. Despite the weakness of the emission, generally detected using photon-counting techniques, the optical nature of the detection permitted local spectroscopic studies of rough metal surfaces [7,8] or single silver clusters [9].

An elementary electromagnetic source term consists in a current vector $\boldsymbol{j}(\omega, \boldsymbol{M})$ at frequency ω highly localized around a given point $\boldsymbol{M}_0$. The localized DC tunnel current in a STM arises from the overlap between the evanescent wave functions of filled initial tip electronic state φ_i with energy E_i and empty final sample state φ_f at the same energy. However, each tip state overlaps also with sample states at energies E_f different from E_i, giving rise to AC currents at frequency $\omega = (E_f - E_i)/\hbar$ as sketched in Fig. 2. From a quantum point of view this corresponds to inelastic tunneling from φ_i to φ_f, with simultaneous excitation of an electromagnetic eigenmode. The intensity of those AC currents is a function of the local density

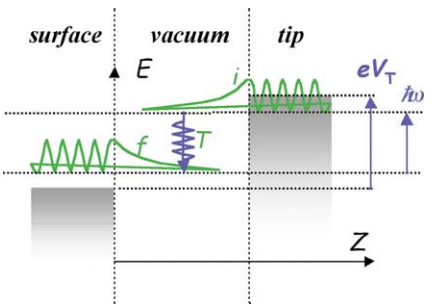

Figure 2. Energy diagram for the inelastic tunneling process of electrons from a metal STM tip (right) to metal-sample surface (left) through a vacuum gap (middle). The maximum energy $\hbar\omega$ of the excited electro-magnetic mode is imposed by the bias, eV_T.

of contributing φ_i and φ_f states at energies E_i and E_f and of the tunneling matrix element T_{if} between them in the tunneling Hamiltonian formalism [1]. The cutoff frequency ω_C is determined by the bias V_T as $\omega_C = eV_T/\hbar$. In metals, both density of states and matrix elements can be approximated as constants over the energy range thus defined. The spectrum of AC currents is fully determined by the DC resistance R of the tunnel junction [1] which is usually kept constant during the scan in STM imaging (so-called constant-current mode or Z mode). However, if other materials are involved, the spectrum of AC currents can be strongly affected by highly structured density of states. For example, in semiconductor samples there are no available empty states φ_f at energy E_f below the gap. The inelastic tunneling process is thus not efficient for moderate biases. However, for p-type direct-gap semiconductors, the tunneling from tip to the conduction band can still generate a luminescence from subsequent electron-hole recombination. The localization of this two-step process may be affected by diffusion of charge carriers prior to recombination.

Then, the elementary source $\boldsymbol{j}(\omega, \boldsymbol{M})$ located around a point $\boldsymbol{M}_0$ will radiate energy through coupling with a given electromagnetic eigenmode at the same frequency. This coupling depends on the amplitude of the electric field of the excited mode at point $\boldsymbol{M}_0$ [10]. The proximity of highly polarizable systems such as metal aggregates or conjugated molecules will thus strongly affect the efficiency of electron–photon conversion. On metal surfaces, the tip itself strongly favors light emission efficiency through the formation of a tip-induced plasmon mode (also called 'gap-mode' [11]), highly localized at the tip-surface junction. When the tip scans the sample, the photon emission variations reflect additional variations of the excited electromagnetic mode due to local perturbations. The first example presented below illustrates this phenomenon.

Enhancements by several orders of magnitude of photophysical processes, such as surface-enhanced raman scattering (SERS) [12], have been observed at rough noble-metal surfaces. The amplification role played by local field enhancements, especially in plasmon oscillation modes, is now clearly established [13]. Further insights in the microscopic mechanisms of plasmon-mediated processes can be gained by applying STM-induced luminescence on model systems with well-controlled geometry [14]. A particularly interesting system consists in thiol-molecule coated silver nanoparticles [15]. For low size dispersities, these nanoparticles self-assemble at room temperature as two-dimensional monolayers on an atomically flat (111) gold surface [16].

3. Experimental setup and STM results

To measure STM-induced measurements, a light collection optics must be adapted to the STM. In our laboratory, it consists in a high-numerical-aperture lens either under Ultra-High Vacuum (UHV) [14] or at air [17]. However, several alternative geometries have been reported in the literature. The detection axis is close to the grazing incidence, at about 75° from the surface normal. The emitted light is focused (in UHV through a view port) onto an avalanche photodiode, operating in a photon-counting mode. Photon maps are acquired simultaneously with topographic maps using home-made electronics. Photon counts are recorded

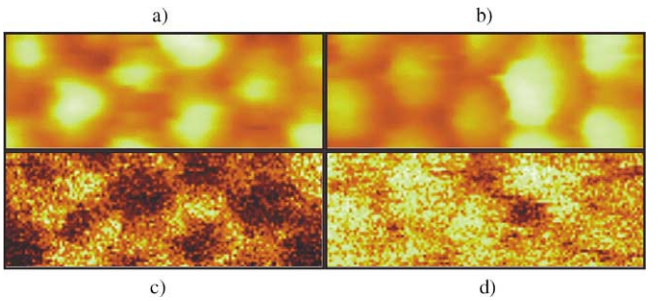

Figure 3. Simultaneously recorded STM topography ((a), (b)) and photon map ((c), (d)) for self-assembled thiol-coated silver particles. Scan area 26×10 nm^2, sample bias $V_S = 2.0$ V ((a), (c)) and 2.5 V ((b), (d)). Set-point current $I_T = 3.5$ nA.

at each pixel for a fixed acquisition time. The STM operates in constant-current mode and either gold or platinum–iridium STM tips are used.

A closeup (26×10 nm^2) of a self-assembled domain is presented in Fig. 3 (from [14]). The topography (Fig. 3, (a) and (b)) and the photon maps (Fig. 3, (c) and (d)) were recorded simultaneously. Images on Fig. 3, (a)–(d), were recorded on the same area using different biases: $V_T = 2.0$ V ((a), (c)) and $V_T = 2.5$ V ((b), (d)). In both cases, the tunnel current was set to 3.5 nA. Although apparent topographies (Fig. 3, (a) and (b)) are similar, the photon maps (Fig. 3, (c) and (d)) exhibit drastic differences in photon emission efficiencies: at the lower bias (2.1 V, Fig. 3, (a) and (c)), light emission is below the detection limit when the tip is located above the top of a particle whereas a maximum is reached between particles. In contrast, when a bias of 2.5 V (Fig. 3, (b) and (d)) is applied, the maximum of photon emission is detected on the top of the particle and the minimum is attained when the tip is above a junction between two particles. Electrons always tunnel toward silver. We can thus assume low variations of electronic structure during the scan. The formation of tip-induced mode results from the interaction of the tip apex with sample modes. Hence, the observed changes in photon emission rate during constant–current scanning mainly map the sample modes which, participate to the excited modes at a given bias. Then, the observed variations can be understood in terms of the collective plasmon modes of the hexagonal silver-particle network [14]. In particular the enhancement between particles at lowest bias reflects the lowest-energy mode of a simple two-particle model, which mainly consists in a gap-mode localized between them [18]. Analysis of STM-induced luminescence thus permits one to analyse the effects of local geometry on photonic processes. Tuning the STM bias makes possible an excitation spectroscopy. The understanding of the collective excitations in such a system may lead to a control of field distribution and optimization of photonic properties at the nanoscale.

4. Dynamical experiments

Despite a good ordering into a hexagonal network, the quantum efficiencies of STM-induced luminescence of single nanoparticles appears highly site dependent [19]. As shown in the cross sections in Fig. 4, the STM-induced luminescence of some specific particles appear completely quenched. This behavior has been correlated with an increased mobility of such ‘dark’ particles within their hexagonal site [19]. In the particular case represented in Fig. 4, moreover, a ‘dark’ particle is located next to a vacant site. The STM tip can also be used to manipulate individual nano-scale objects at the single atoms [20] or single molecule [21] level at low temperature. Room temperature manipulation and control of the nanoparticle assembly at the single-particle scale can be realized through direct mechanical interactions with the sharp STM tip by increasing tunnel-current set-point [22].

The switching of the luminescence of the ‘dark’ particle through STM manipulation is reported in Fig. 4, presenting the tip height curves during the moving of a single particle with simultaneously recorded STM induced light emission. The particle is first located at site A at time T_0. It is then moved toward the vacant neighbor site B by a right-to-left scan of the STM tip at T_1. As a consequence of this displacement the luminescence of the particle is nearly completely switched off. It is then switched on and off successively by

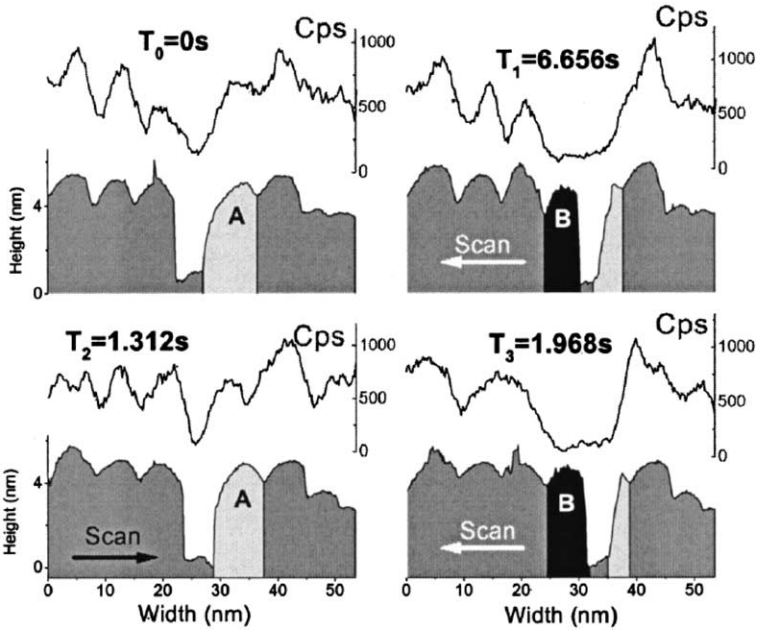

Figure 4. Cross section of STM topography and corresponding photon emission curve during three successive particle manipulations, sample bias: $V_T = 2.5$ V; tunnel-current set-point: $I_T = 5.3$ nA. Particle was alternatively shifted through action of the STM tip between luminescent site A (light gray area) and site B (black area) where the light emission is quenched.

moving the particle into site A and B at times T_2 and T_3. The process has been successively repeated about 10 times before the image was lost, due to drift in piezoelectric motion. These observations demonstrate that luminescence quenching does not depend on the particle itself but on the site where it lies. Two mechanisms of this site-dependent quenching may be invoked. The first one involves variations in the height of a second tunnel-barrier between tip and substrate. This could be caused by an inhomogeneous coverage of the gold surface by some alkanethiols molecules separated from silver particles. The reduced tip-particle junction resistance would then result in an increased mechanical influence of the tip on the particle, consistent with the observations. A second possibility involves the electron–phonon dynamics in the metal nanoparticle network. An increased particle mobility could open additional inelastic-tunneling channels with excitation of local phonon modes instead of the radiative optical mode. These results provide evidence for the realization of a light-emission switch with high reversibility, at nanometer scale and at room temperature. Here, STM was used for imaging, manipulating and excitating the luminescence of single nanoparticle.

5. Molecular excitation

The next challenge in this technique is the excitation of individual molecules. A first demonstration of molecular-scale contrasts in photon maps was achieved on C_{60} molecules deposited on gold [4]. The influence of a the organization of a monomolecular layer on STM-induced luminescence has been demonstrated recently on self-assembled alkane-thiol molecules attached to a gold surface [23]. At first sight, the use of intrinsically luminescent molecules such as conjugated luminophores is an attractive route. However the quantum efficiency of such luminophores close to conducting materials is low, and large current densities are still needed. Such current densities very rapidly damage the conjugated layer. To illustrate this effect, we report on Fig. 5 the effect of scanning under luminescence conditions on a terthiophene-functionalized thiol monolayer. The continuity of gold monoatomic step edges crossing the damaged square region shows that the underlying gold substrate has not been affected. The surface changes, as imaged by STM, thus result from damage to the molecular layer, most probably a bleaching of the conjugated moiety of the self-assembled molecules.

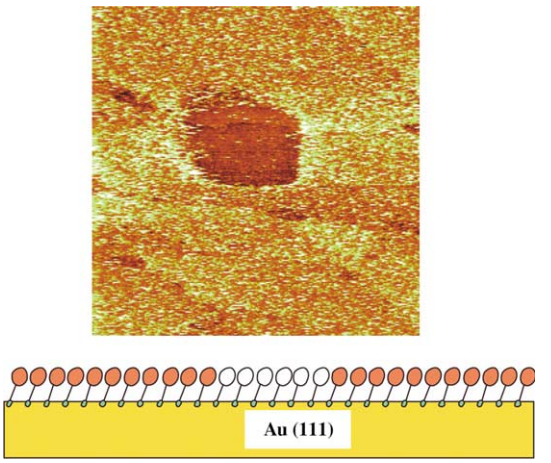

Figure 5. STM image of a 500 × 500 nm^2 self-assembled terthiophene-substituted alkane-thiol monolayer on gold (111) epitaxially grown on mica (low bias and current). A 90 × 90 nm^2 area in the center of the image was previously scanned in light-emission conditions ($V_T = 3.2$ V, $I_T = 200$ pA).

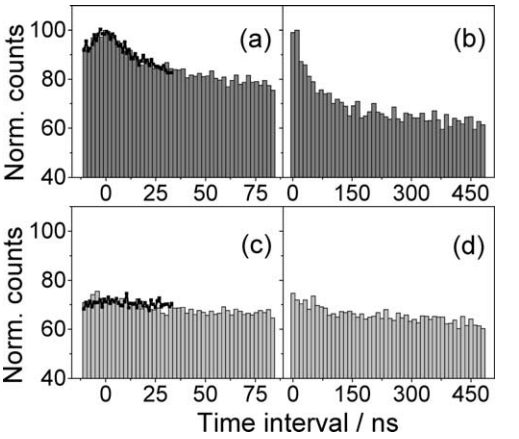

Figure 6. Histograms of recorded time intervals between consecutive pairs of detected photons for two different bias voltages applied on the substrate: 2.5 V ((a), (b)) and 2.0 V ((c), (d)). The results obtained with TAC time ranges of 50 nm (solid squares) and 100 ns (bars) are superimposed for each bias: (a) 2.5 V and (c) 2.0 V. The histograms obtained with a range of 500 ns are represented on a larger scale for each bias: (b) 2.5 and (d) 2.0 V.

6. Time resolved photon counting

One unique opportunity offered by optical detection is time-resolution down to ultrafast time-scales. According to the simple probabilistic mechanism of the STM-luminescence described above, for stable samples, individual photon emission events are independent one from another, leading to randomly distributed photon-emission times. However, in more complex systems, dynamic electronic or structural effects could take place. Moreover the mechanisms of STM induced photon emission may deviate from this simple model. Then the time statistics of single-photon emissions can be completely different. As an example, a time-resolved detection of STM-excited luminescence of polymer light-emitting diodes has allowed us to detect photon bunches in the millisecond time scale attributable to high-field avalanche processes [24]. Thus, in contrast to extended light sources, the highly local nature of the STM-induced luminescence makes possible strong correlations between successive single-photon emission events, as, for example, bunching or antibunching phenomena. Such photon correlations are intimately connected to the dynamics of the source that produced them [25]. The analysis of time correlations in single-photon detection can then give valuable information on the dynamic processes taking place after tip-induced excitation.

Time-autocorrelated two-photon counting measurements have been successfully applied to the study of time correlations in laser-excited systems such as such, e.g., few-molecule fluorescence [26]. Recently, we used this technique to study STM-induced photon emission, with time resolutions down to the nanosecond time scale. For this purpose, the collected light is split symmetrically between two detectors connected to the start and stop inputs of a time-to-amplitude converter (TAC). Time intervals between single-photon detection can be measured with an accuracy better than 200 ps. For each event, which consists in the detection of a valid start-and-stop pulse pair, the electronic system records the measured time interval, the current X–Y coordinates of the scanning tip. These data are stored for each individual event for subsequent off-operation statistical treatments. This permits one to generate histograms of the start-stop time intervals acquired on a selected area as well as maps of mean time intervals measured simultaneously with STM topography.

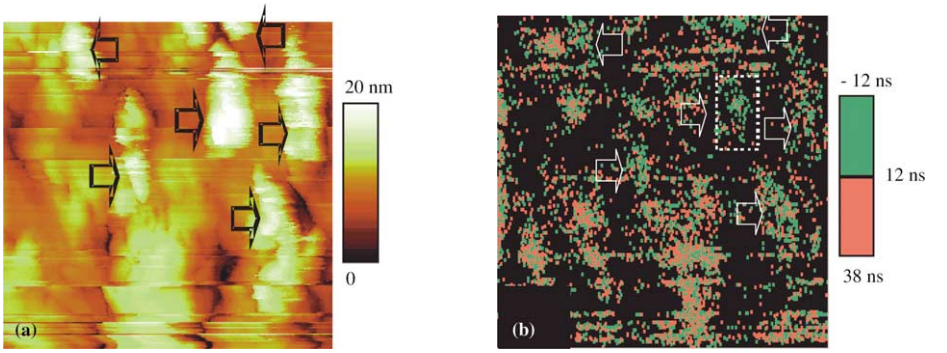

Figure 7. Simultaneously recorded topography of a rough gold surface (a) and map of time-autocorrelated two-photon events (b). Time interval belonging to [−12 ns, 12 ns] are represented in green, whereas those belonging to [+12 ns, 38 ns] are represented in pink. Image dimensions: 250 nm×250 nm. ($V_T = 2.0$ V, $I_T = 1.5$ nA).

In the case of a gold surface at air, light emission exhibits a strong bunching behavior at the nanosecond scale for a bias of 2.5 V as reported on the histograms of Fig. 6, (a) and (b). The bunching peak width corresponds to a time constant of the order of 12 ns. Moreover this two-photon time correlation appears strongly bias dependent in the voltage range 2.0–2.5 V, since no such correlation appears when the voltage is decreased to 2.0 V (Fig. 6, (c) and (d)).

The relationship between such photon correlation and the local topography is expected to give crucial information on both electronic and structural fast dynamic processes taking place locally at surfaces. The map of two-photon auto-correlations on a 50-ns time scale is represented on Fig. 7, together with the topography, in the case of a rough gold surface at air. Time correlations appear as a new contrast mechanism for scanning probe microscopy. As a matter of fact the bunching phenomenon present at biases near 2.5 V appears strongly spatially dependent. More precisely it is present exclusively at specific less emissive bumps of the gold surface, indicated by arrows on both topography and correlation maps. The similarity between the conditions for observation of bunching and some tip-induced surface modifications observed previously [27,28] suggest that this effect could be a manifestation of a diffusion-controlled reorganisation of tip-induced transient atomic-scale defects. Optical diagnostics then permits measurements of the dynamics of tip-induced defects at unprecedented time resolutions compared with other surface-characterization techniques. Moreover, observations of time-correlations in such down-scaled light sources opens opportunities in nanophotonics for addressing and triggering single photon sources which would exhibit non-classical behaviors, such as single molecules or quantum dots.

7. Conclusions

In conclusion, in STM-induced luminescence experiments, the STM tip is used simultaneously as a tunnel-current probe to map the topography of the studied sample and as a highly-localized excitation source generating luminescence. A third possible simultaneous action of the tip is the modification of the surface. We have illustrated this possibility here for the reversible reorganization of a self-assembled nanoparticle monolayer, the local bleaching of self-assembled dye-functionalized monomolecular layers, or the transient effects of a biased tip at air on gold surfaces. The simultaneous influence of such tip-induced effects on both nano-scale topography and locally-excited luminescence gives very valuable informations on the fundamental photonic processes taking place at molecular-scale level. As compared with other surface characterization techniques, optical detection coupled to the STM offers a very powerful local diagnostic tool through the possibility of optical spectroscopy. We have illustrated these new possibilities here in the case of time resolution.

The next challenges are to search for a better understanding of fundamental processes leading to luminescence at the nanoscale, and the excitation of individual quantum objects such as semiconductor quantum dots or conjugated molecules thus forming highly-correlated nanoscale light sources. The observation of STM-induced luminescence at a liquid–solid interface [29] may offer new perspectives to address individual molecules. In fact, some conjugated molecules can form stable self-assembled monolayers at a liquid–solid interface which can be probed by STM with intramolecular resolution [30].

[1] Present address: Université de Lausanne, IPMC, CH-1015 Lausanne, Switzerland.

Acknowledgements. The results on terthiophene-functionalized thiol self-assembled monolayers were obtained in collaboration with A. Yassar and D. Fichou, from LMM, CNRS Thiais, France. The work on silver nanoparticles is a colaboration with A. Taleb and M.-P. Pileni, from LM2N, Paris VI University, France.

References

[1] R.W. Rendell, D.J. Scalapino, Phys. Rev. B 24 (1981) 3276.
[2] J. Lambe, S.L. McCarthy, Phys. Rev. Lett. 37 (1976) 923.
[3] J.K. Gimzewski, J.K. Sass, R.R. Schlitter, J. Schott, Europhys. Lett. 8 (1989) 435.
[4] R. Berndt, R. Gaisch, J.K. Gimzewski, B. Reihl, R.R. Schlitter, W.D. Schneider, M. Tschudy, Science 262 (1993) 1425.
[5] A. Downes, M.E. Welland, Phys. Rev. Lett. 81 (1998) 1857.
[6] C. Thirstrup, M. Sakurai, K. Stokbro, M. Aono, Phys. Rev. Lett. 82 (1999) 1241.
[7] M.M.J. Bischoff, M.C.M.M. van der Wielen, H. van Kempen, Surf. Sci. 400 (1998) 127.
[8] K. Ito, S. Ohyama, Y. Uehara, S. Ushioda, Surf. Sci. 324 (1995) 282.
[9] P. Dumas, C. Syrykh, I.V. Makarenko, F. Salvan, Europhys. Lett. 40 (1997) 447.
[10] P. Johansson, R. Monreal, P. Apell, Phys. Rev. B 42 (1990) 9210.
[11] A.G. Mal'shukov, Phys. Rep. 194 (1990) 343.
[12] M. Moskovits, Rev. Mod. Phys. 57 (1985) 783.
[13] F.J. García-Vidal, J.B. Pendry, Phys. Rev. Lett. 77 (1996) 1163.
[14] F. Silly, A.O. Gusev, A. Taleb, F. Charra, M.-P. Pileni, Phys. Rev. Lett. 84 (2000) 5840.
[15] A. Taleb, C. Petit, M.P. Pileni, Chem. Mater. 9 (1997) 950.
[16] A. Taleb, C. Petit, M.P. Pileni, J. Phys. Chem. 102 (1998) 2214.
[17] F. Silly, F. Charra, Appl. Phys. Lett. 77 (2000) 3648.
[18] H. Xu, J. Aizpurua, M. Käll, P. Apell, Phys. Rev. E 62 (2000).
[19] A.O. Gusev, F. Silly, A. Taleb, F. Charra, M.P. Pileni, Adv. Mater. 12 (2000) 1583.
[20] D.M. Eigler, C.P. Lutz, W.E. Rudge, Nature 352 (1994) 600.
[21] F. Kulzer, S. Kummer, R. Matzke, C. Brauchle, Th. Basche, Nature 387 (1997) 688.
[22] F. Silly, A.O. Gusev, F. Charra, A. Taleb, M.-P. Pileni, Appl. Phys. Lett. 79 (2001) 4013.
[23] G.E. Poirier, Phys. Rev. Lett. 86 (2001) 83.
[24] F. Charra, S. Bouchel, O. Plessis, J.-M. Nunzi, P. Raimond, C. Denis, E. Gautier-Thianche, Opt. Mater. 12 (1999) 249.
[25] R. Loudon, Quantum Theory of Light, Oxford University Press, Oxford, 1983, Chapters 3 and 6.
[26] S.C. Kitson, P. Jonsson, J.G. Rarity, P.R. Tapster, Phys. Rev. A 58 (1998) 620.
[27] V. Sivel, R. Coratger, F. Ajustron, J. Beauvilain, Phys. Rev. B 51 (1995) 14598.
[28] Y. Uehara, T. Fujita, S. Ushioda, Phys. Rev. Lett. 83 (1999) 2445.
[29] R. Nishitani, A. Kasuya, Surf. Science 435 (1999) 283.
[30] F. Charra, J. Cousty, Phys. Rev. Lett. 80 (1998) 1682.